

5 STRESS-LIFE (S-N) CURVES

5.1 General S-N Behavior

Two typical schematic S-N curves obtained under axial load or stress control test conditions with smooth specimens are shown in Fig. 6. Here S is the applied nominal stress, usually taken as the alternating stress, σ_a , and N_f is the number of cycles or life to failure, where failure is defined as fracture. The constant amplitude S-N curves of these types are plotted on semilog or log-log coordinates and often contain fewer data points than shown in Fig. 6b. S-N curves obtained under torsion or bending load-control test conditions often do not have data at the shorter fatigue lives (say, 10^3 or 10^4 cycles or less) due to significant plastic deformation; the torsion and bending stress equations can be used only for nominal elastic behavior. Figure 6b shows typical variability, with less variability in life at the shorter lives and greater variability in life at the longer lives. From Fig. 6b, the variability in life for a given stress level can range from less than a factor of 2 to more than one or two orders of magnitude.

Figure 6a shows a continuously sloping curve, while Fig. 6b shows a discontinuity or “knee” in the S-N curve. This knee has been found in only a few materials (notably the low- and medium-strength steels) between 10^6 and 10^7 cycles under noncorrosive conditions. Most materials do not contain a knee even under carefully controlled environmental conditions. In corrosive environments all S-N data invariably have a continuously sloping curve. When sufficient data are taken at several stress levels, S-N curves are usually drawn through median lives and thus represent 50 percent expected failures. Common terms used with the S-N diagram are “fatigue life,” “fatigue strength,” and “fatigue limit”.

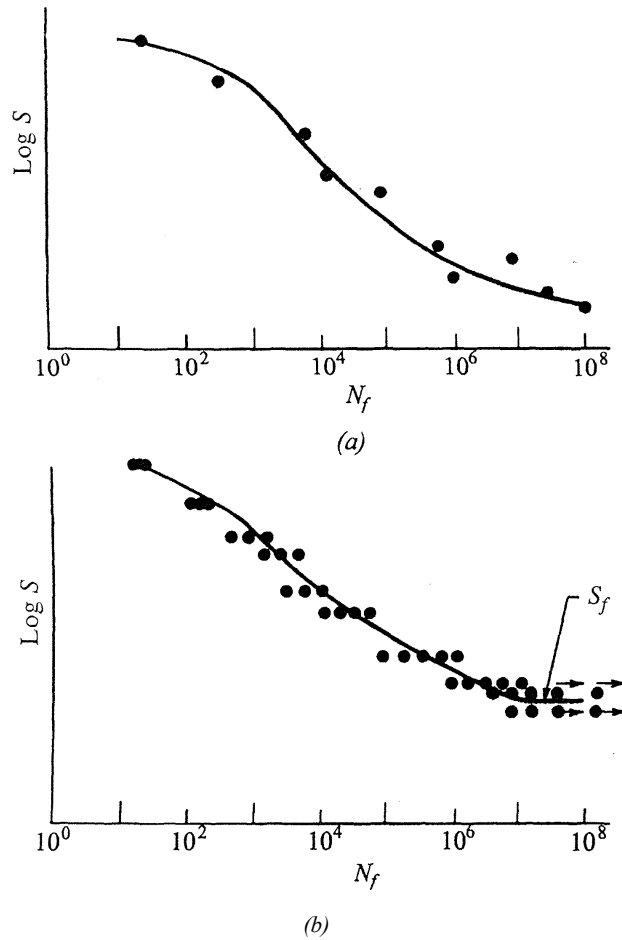


Fig. 6 Typical S - N diagrams

The fatigue life, N_f , is the number of cycles of stress or strain of a specified character that a given specimen sustains before failure of a specified nature occurs. Fatigue strength, σ_N , is a hypothetical value of stress at failure for exactly N_f cycles, as determined from an S - N diagram. The fatigue limit, is the limiting value of the median fatigue strength as N_f becomes, very large. The above definitions are all based on median lives or 50 percent survival.

In Chapter 4 it was emphasized that fatigue typically consists of crack nucleation, growth, and final fracture. Figure 6 does not separate crack nucleation from growth, and only the total life to fracture is given. Let us assume a reasonable crack nucleation life defined by a crack length of 0.25 mm. This dimension, which is easily seen at 10X to 20X magnification, can relate to engineering dimensions and can represent a small macro-crack. The number of cycles required to form this small crack in smooth, unnotched or notched fatigue specimens and components can range from a small percentage to almost the entire life. This is illustrated schematically in Fig. 7, where

applied stress amplitude is plotted versus number of cycles to failure (fracture) and number of cycles to crack nucleation. Linear scales are implied so as not to disguise axis compression due to log-log scales. Here it is seen that a larger fraction of life for crack growth, the hatched area, occurs at higher stress levels, while a larger fraction of life for crack nucleation occurs at lower stress levels. Based on many factors covered in this book, fatigue crack nucleation, growth, and final fracture lives can be significantly altered. When fatigue crack growth life is significant, then fracture mechanics should be used. The size of the final crack at fracture depends on the fracture toughness of the material and the stress level. The higher stress levels have shorter critical crack sizes and the lower stress levels have larger critical crack sizes. Assuming that test specimens are between 3 and 10 mm in diameter, and that critical crack lengths can vary from 10 to 50 percent of the diameter, critical crack lengths for these small test specimens vary from about 0.25 to 5 mm.

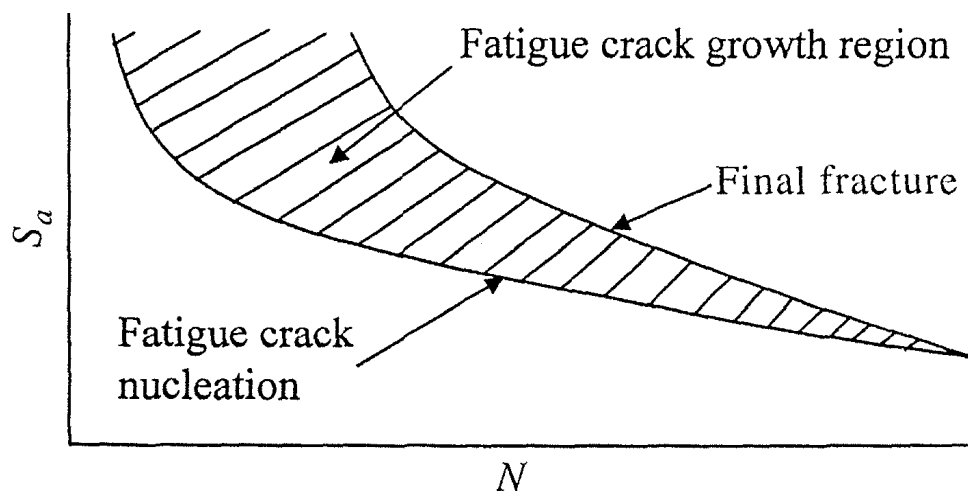


Fig. 7 S-N schematic of fatigue crack nucleation, growth, and final fracture

5.1.1 Fatigue Limit Under Fully Reversed Uniaxial Stressing

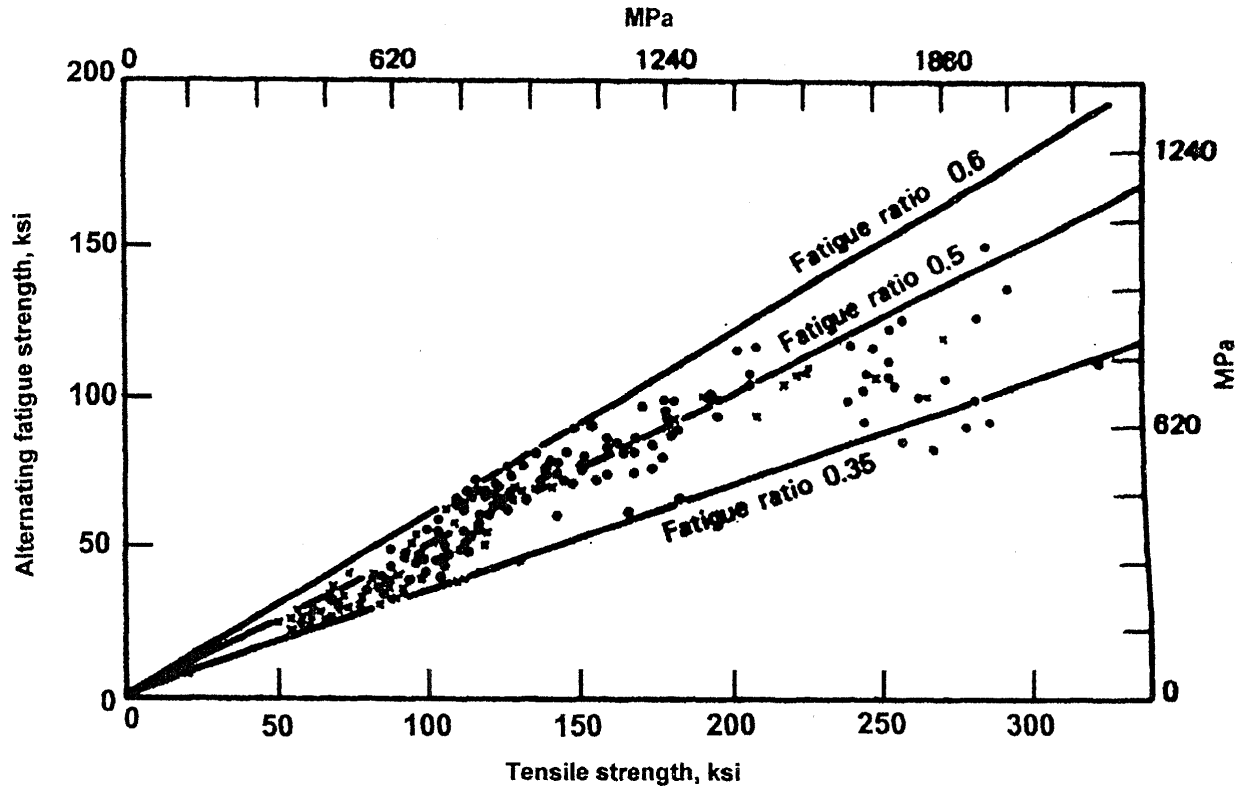
The fatigue limit has historically been a prime consideration in long-life fatigue design. For a given material the fatigue limit has an enormous range, depending on surface finish, specimen or component size, type of loading, temperature, corrosive and other aggressive environments, mean stresses, residual stresses, and stress concentrations. Considering the fatigue limit based on a nominal alternating stress, σ_a ,

this value has ranged from essentially 1 to 70 percent of the ultimate tensile strength. An example of a case in which the fatigue limit may be approximately 1 percent of σ_b is a high-strength steel with a sharp notch subjected to a high mean tensile stress in a very corrosive atmosphere. An example of a case in which the fatigue limit might approach 70 percent of σ_b is a medium-strength steel, in an inert atmosphere, containing appreciable compressive residual stresses.

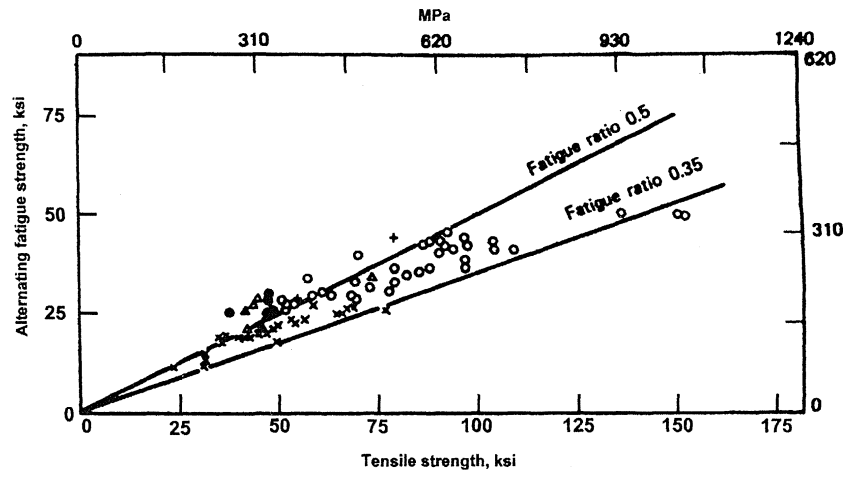
Most long-life $S-N$ fatigue data available in the literature consist of fully reversed ($\sigma_m = 0$) uniaxial fatigue strengths or fatigue limits of small, highly polished, unnotched specimens based on 10^6 to $5 \cdot 10^8$ cycles to failure in laboratory air environment.

A common procedure to partially compare materials for their fatigue resistance is to plot the unnotched, fully reversed fatigue limit, σ_f , obtained under similar ideal laboratory conditions described above versus the ultimate tensile strength, σ_b . The σ_f / σ_b ratio is called the “fatigue ratio”.

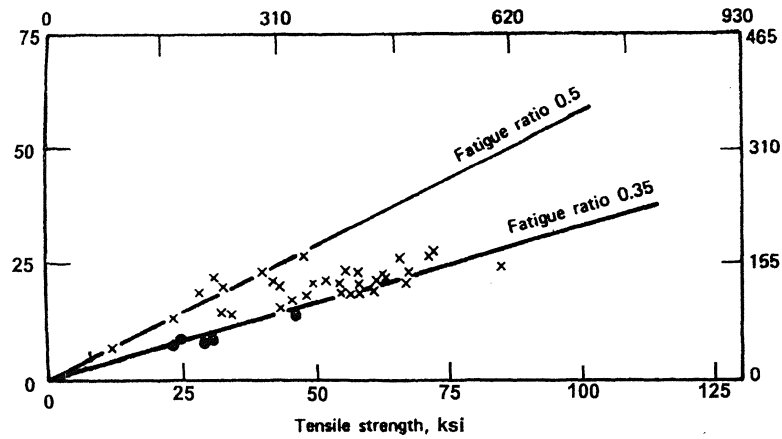
Figure 8 shows plots for many tests of steels, irons, aluminum alloys, and copper alloys subjected to rotating bending tests with fatigue limits or fatigue strengths based on 10^7 to 10^8 cycles. Lines of constant fatigue ratio, σ_f / σ_b , equal to 0.35, 0.5, and 0.6 are superimposed on data in Fig. 8a, and 0.35 and 0.5 fatigue ratio lines are superimposed on data in Figs. 8b-d. It is quite clear that σ_f / σ_b varies from about 0.25 to 0.65 for these data. There is a tendency to generalize that σ_f increases linearly with σ_b . A careful examination of Fig. 8 shows that this is incorrect and that data bands tend to bend over at the higher ultimate strengths. This undesirable tendency, however, can be minimized by suitable mechanical or thermal surface treatment. Also, for more recent cleaner high-strength steels ($\sigma_b > 1400$ MPa), the fatigue limit is not as low as shown in Fig. 8a due to fewer inclusions and other impurities and hence fewer crack nucleation sites. The fatigue resistance of these cleaner steels depends more on material strength than on inclusion/porosity content.



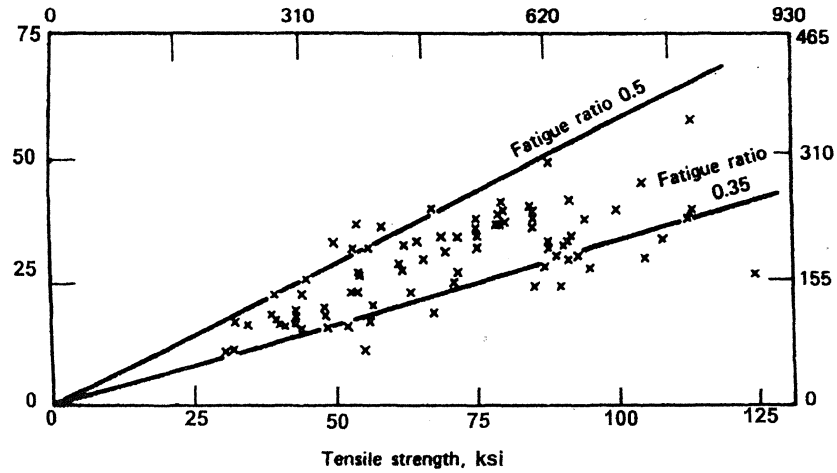
(a)



(b)



(c)



(d)

Fig. 8. Relation between bending unnotched fatigue strength and ultimate tensile strength, (a) Carbon and alloy steels (10^7 to 10^8 cycles): (•) alloy steels, (x) carbon steels. (b) Wrought and cast irons (10^7 cycles): (x) flake-graphite cast iron, (O) nodular cast iron, (+) malleable cast iron, (Δ) ingot iron, (•) wrought iron, (c) Aluminum alloys (10^8 cycles): (x) wrought, (•) cast, (d) Wrought copper alloys.

Figure 8a for steels indicates that substantial data are clustered near the fatigue ratio $\sigma_f / \sigma_b \sim 0.5$ for the low- and medium-strength steels. The data, however, actually fall between 0.35 and 0.6 for $\sigma_b < 1400$ MPa. For $\sigma_b > 1400$ MPa, σ_f does not increase significantly. Thus, very common, loosely used estimates for unnotched, highly polished, small bending specimen fatigue limits for steels are

$$\sigma_f \approx 0.5 \sigma_b \text{ for } \sigma_b < 1400 \text{ MPa} \quad (3a)$$

$$\sigma_f \approx 700 \text{ MPa for } \sigma_b > 1400 \text{ MPa} \quad (3b)$$

For steels, σ_b can be approximated from the Brinell hardness (HB) as

$$\sigma_b \sim 8.45HB \text{ for MPa units} \quad (4a)$$

Other similar $\sigma_b - HB$ empirical formulas have been suggested, and data indicate that the above popular relations can be quite accurate and also can have a 10 to 20 percent error. HB values above 400 in Eq. 4 often give σ_b values 10 to 15 percent lower than actual values. By suitable mechanical or thermal surface treatments, fatigue limits of high-strength steels can be increased to agree more with Eq. 3a. Equations 3 are not unreasonable for the small, highly polished steel specimens tested, but empirical

reduction factors for surface finish, size, stress concentration, temperature, and corrosion must also be considered. We strongly warn against using a design fatigue limit equal to one-half of the ultimate strength of steels. Most data in Fig. 8 for irons, aluminum, and copper alloys fall below the 0.5 fatigue ratio. The aluminum and copper alloy data bands bend over at higher strengths, as do the bands for steels. Thus, high-strength steels, aluminum, and copper alloys generally do not exhibit correspondingly high unnotched fatigue limits.

Data for steels similar to those in Fig. 8a can be generalized into schematic scatter bands, as shown in Fig. 9. Here it is also seen that severely notched and/or corroding specimens have substantially lower fatigue limits than unnotched specimens. This behavior has too often been given insufficient importance in fatigue design. But again, this can be significantly altered in many cases by proper mechanical or thermal surface treatment.

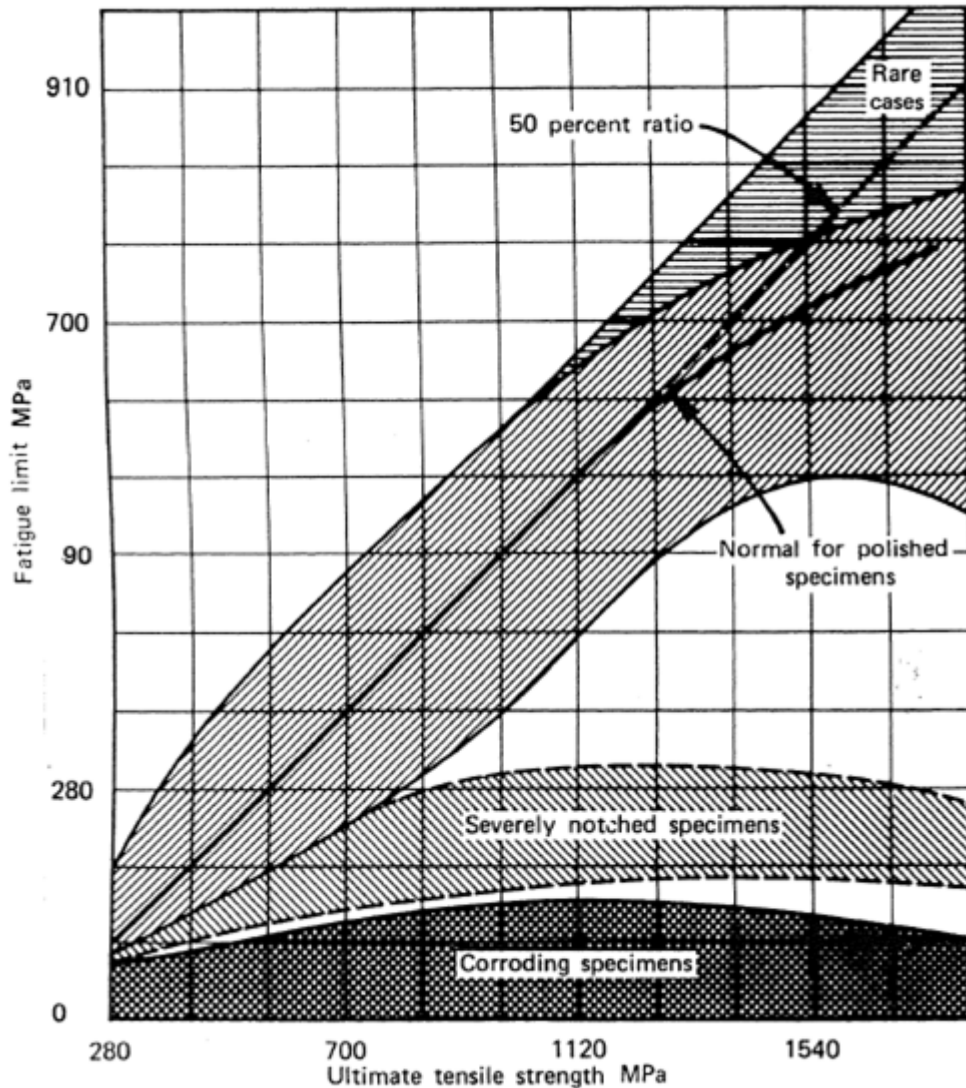


Figure 9 General relationship between fatigue limit and tensile strength for polished unnotched, notched, and corroding steel specimens.

5.2 MEAN STRESS EFFECTS ON S-N BEHAVIOR

The alternating stress, σ_a , and the mean stress, σ_m , are defined in Fig. 2. The mean stress, σ_m , can have a substantial influence on fatigue behavior. This is shown in Fig. 10, where alternating stress, σ_a , is plotted against the number of cycles to failure, N_f , for different mean stresses. It is seen that, in general, tensile mean stresses are detrimental and compressive mean stresses are beneficial. This is also shown by the three vertical lines indicating fatigue life: N_{ft} , N_{f0} , and N_{fc} , representing fatigue life for tensile, zero, and compressive mean stress, respectively, for a given alternating stress, S_a . At

intermediate or high stress levels under load control test conditions, substantial cyclic creep (also referred to as “cyclic ratcheting”), which increases the mean strain, can occur in the presence of mean stresses, as shown in Fig.11. This cyclic creep adds to the detrimental effects of tensile mean stress on fatigue life and results in additional undesirable excess deformation.

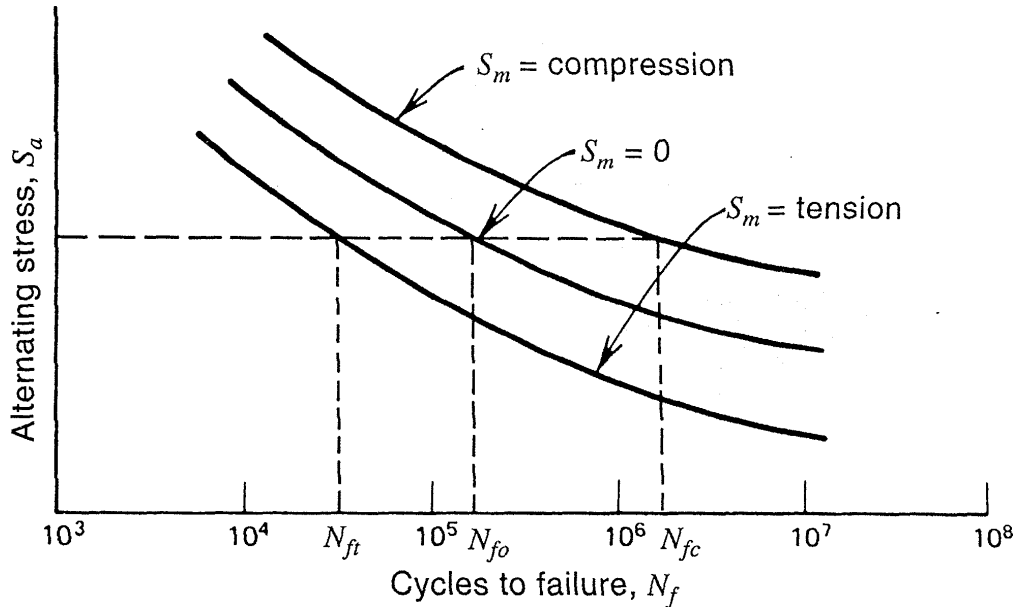


Figure 10. Effect of mean stress on fatigue life.

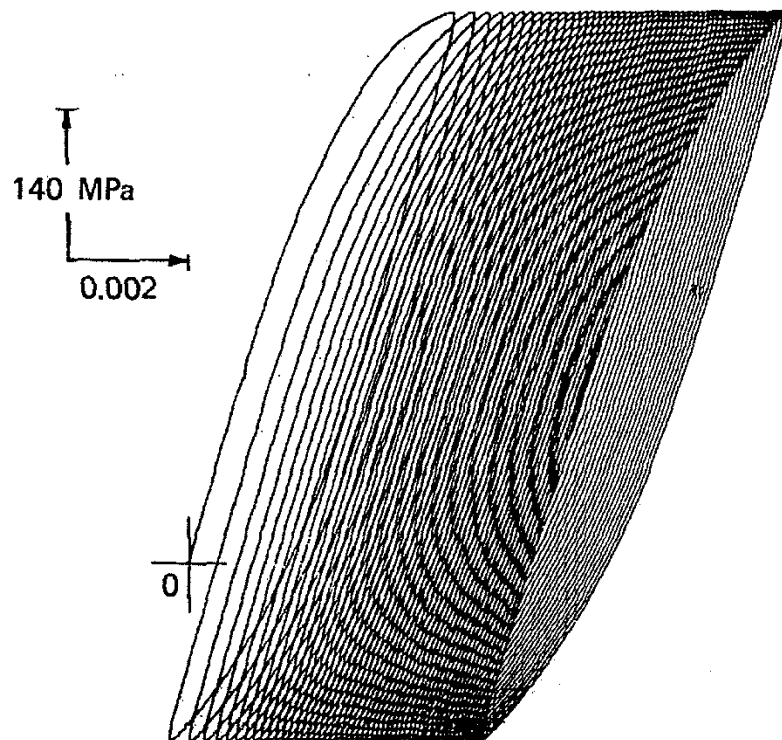
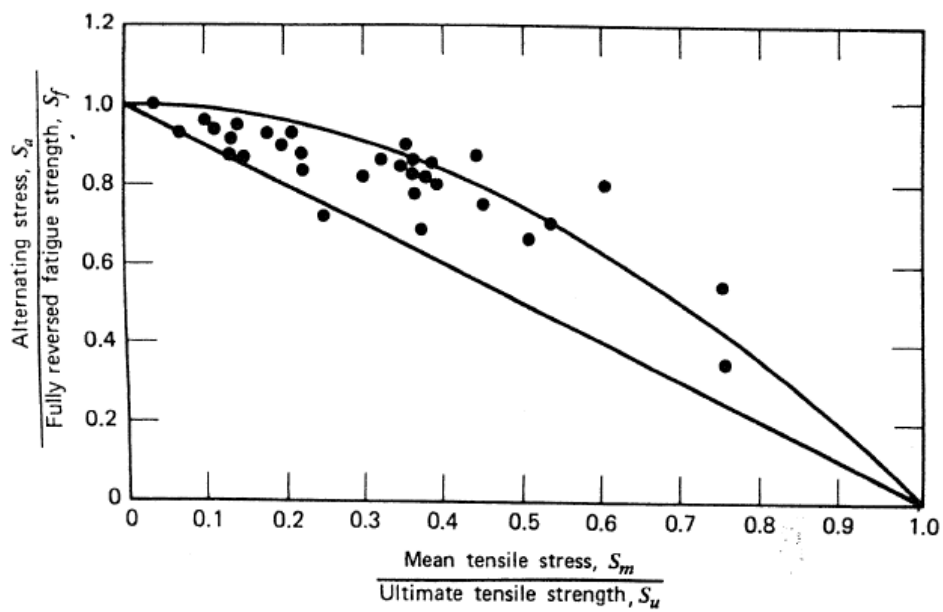
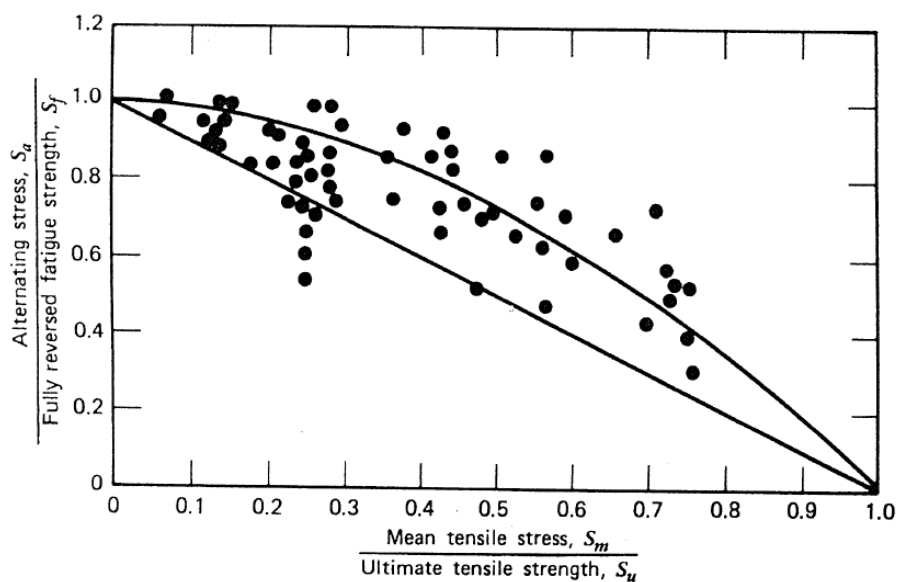


Figure 11. Cyclic creep under load control constant amplitude testing, $\sigma_m > 0$.

Substantial investigation of tensile mean stress influence on long-life fatigue strength has been made. Typical dimensionless plots are shown in Fig. 12 for steels and aluminum alloys, where σ_a/σ_f versus σ_f/σ_b is plotted. σ_f is the fully reversed, ($\sigma_m = 0$, $R = -1$), fatigue limit of smooth specimens, and σ_b is the ultimate tensile strength. Similar behavior exists for other alloys.



(a)



(b)

Figure 4.12 Effect of mean stress on alternating fatigue strength at long life, (a) Steels based on $\sim 10^7$ cycles. (b) Aluminum alloys based on $\sim 5 \cdot 10^7$ cycles.

Substantial scatter exists, but the general trend indicating that tensile mean stresses are detrimental is quite evident. Small tensile mean stresses, however, often have only a small effect. It appears that much of the data fall between the straight and curved lines. The straight line is the modified Goodman line, and the curve is the Gerber parabola. An additional popular relationship has been formulated by replacing σ_b with σ_{ffr} (Morrow line), where σ_{ffr} is the true fracture strength. The following equations represent these tensile mean stress effects for uniaxial state of stress:

$$\text{Modified Goodman:} \quad \frac{\sigma_a}{\sigma_f} + \frac{\sigma_m}{\sigma_b} = 1. \quad (5a)$$

$$\text{Gerber:} \quad \frac{\sigma_a}{\sigma_f} + \left(\frac{\sigma_m}{\sigma_b} \right)^2 = 1. \quad (5b)$$

$$\text{Morrow:} \quad \frac{\sigma_a}{\sigma_f} + \frac{\sigma_m}{\sigma_{ffr}} = 1 \quad (5c)$$

All three expressions have been used in fatigue design when modified for notches, size, surface finish, environmental effects, and finite life. A yield criterion has also been used in conjunction with these expressions.

Figure 4.12 does not provide information on compressive mean stress effects, as shown by in Fig. 13 for several steels and aluminum alloys.

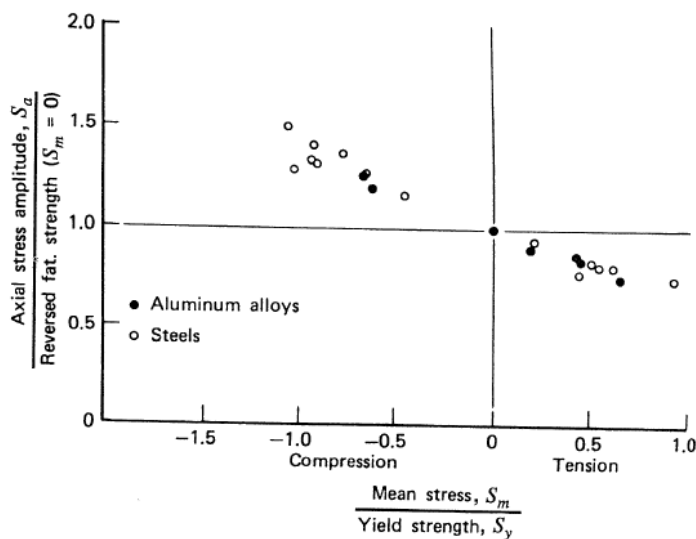


Figure 13. Compressive and tensile mean stress effect. (●) Aluminum alloys, (○) steels

It is seen that these compressive mean stresses cause increases of up to 50 percent in the alternating fatigue strength. Even higher increases have been shown. This increase is too often overlooked, since compressive residual stresses can cause similar beneficial behavior. Based on the fact that compressive mean stresses at long lives are beneficial, the modified Goodman or Morrow equations can be conveniently extrapolated to the compressive mean stress region. The Gerber equation incorrectly predicts a detrimental effect of compressive mean stresses and does not properly represent notched component tensile mean stress fatigue behavior. Thus, we deemphasize the use of the Gerber equation for design. The modified Goodman and Morrow equations are shown in Fig. 14 for a given long life (e.g., $10^6, 10^7, 10^8$ cycles) along with the criterion for uniaxial yielding:

$$\frac{\sigma_a}{\sigma'_y} + \frac{\sigma_m}{\sigma_y} = 1, \quad (6)$$

where σ_y is the monotonic tensile yield strength and σ'_y is the cyclic yield strength. σ_y is used along the σ_m axis since this axis represents monotonic loading only, and σ'_y is used along the σ_a axis since this axis represents the cyclic conditions used to obtain σ_y . If σ'_y is unknown, it can be replaced by σ_y as an approximation.

In fatigue design with constant amplitude loading and unnotched parts, if the coordinates of the applied alternating and mean stresses fall within the modified Goodman or Morrow lines shown in Fig. 14, then fatigue failure should not occur prior to the given life. Note that the difference between the modified Goodman and Morrow equations is often rather small; thus, either model often provides similar results. If yielding is not to occur, then the applied alternating and mean stresses must fall within the two yield lines connecting $\pm \sigma_y$ to σ'_y . If both fatigue failure and yielding are not to occur, then neither criterion, as indicated by the three bold lines in Fig. 14, should be

exceeded. In Fig. 14 the modified Goodman line was used for the bold fatigue line, but the Morrow line could also have been used.

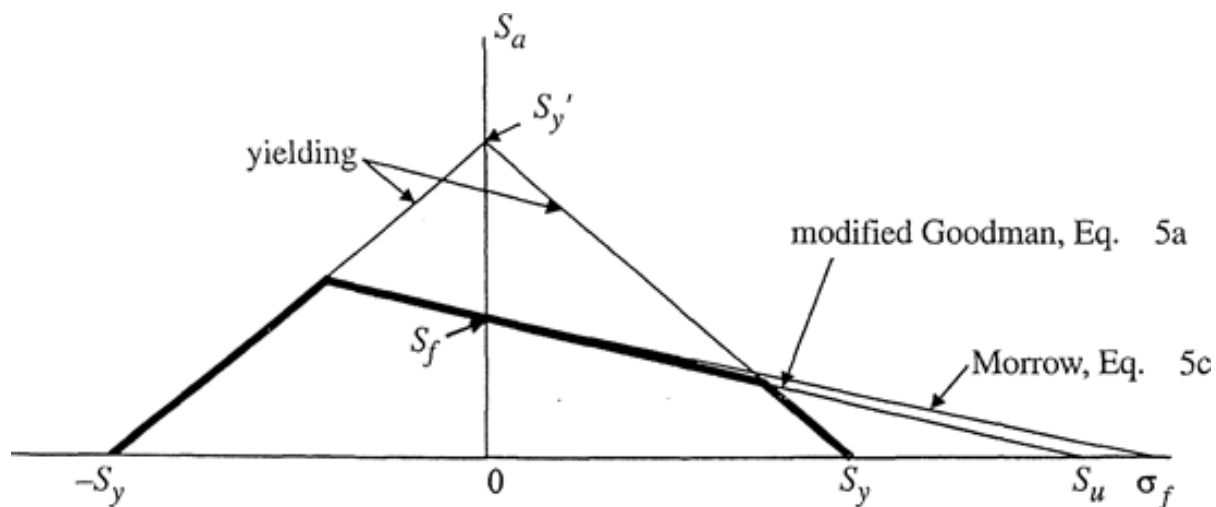


Figure 14 Fatigue and yielding criteria for constant life of unnotched parts

5.1 S-N CURVE REPRESENTATION AND APPROXIMATIONS

Actual fatigue data from either specimens or parts should be used in design if possible. This information may be available through data handbooks, design codes, industry standards, company data files, and previous tests. Often this information is not available and must be generated or approximations of $S-N$ behavior must be made. There are many models depicting $S-N$ curves, and these usually imply a median fatigue life. Figure 16 shows common reasonable $S-N$ median fatigue life curves based upon straight-line log-log approximations.

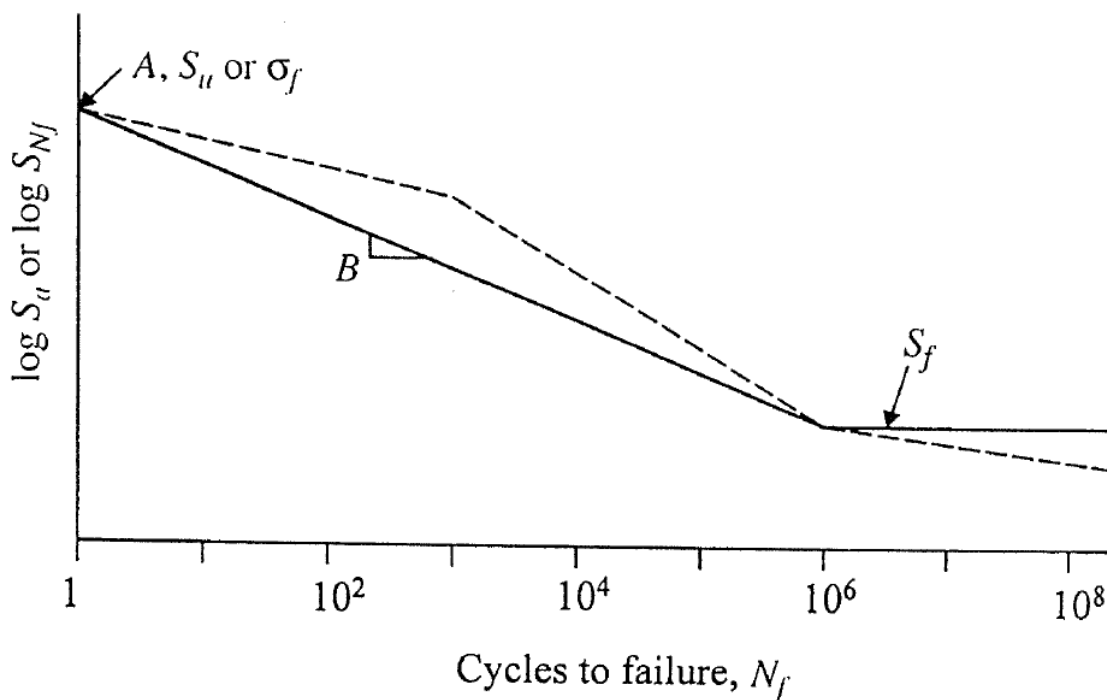


Figure 16. Baskin type S-N curves

Basquin in 1910 suggested a log-log straight line S - N relationship such that

$$\sigma_a \text{ or } \sigma_{N_f} = A \cdot (N_f)^B.$$

where σ_a is an applied alternating stress and σ_{N_f} is the fully reversed, $R = -1$, fatigue strength at N_f cycles, A is the coefficient and represents the value of σ_a or σ_{N_f} at one cycle, and B is the exponent or slope of the log-log S - N curve.

One approximate representation of the median S-N curve is a tri-slope model with one slope between 1 cycle and 10^3 cycles, one slope between 10^3 and 10^6 or 10^8 cycles, and another slope after 10^6 or 10^8 cycles. This model is represented by the dashed lines in Fig. 4.16. The tri-slope model indicates that a fatigue limit does not exist, which may be the case for in-service variable amplitude loading. The tri-slope model exists in some design codes, such as those for gears and welds. In the tri-slope model, the third, or long-life, slope could also be horizontal after 10^6 or 10^8 cycles. Other approximation models assume one sloping straight line from 1 cycle to 10^6 , 10^7 , or 10^8 cycles followed by a horizontal line or another sloped line. The intercept, A , at $N_f = 1$ could be chosen as

the ultimate tensile strength, σ_b , the true fracture strength, σ_f , or an intercept found from regression of the fatigue data.

Often the slope, B , for smooth, unnotched specimens is about -0.1. This suggests that for unnotched specimens the fatigue life is approximately inversely proportional to the 10th power of alternating stress. Thus, a 10 percent increase or decrease in alternating stress will cause a decrease or increase, respectively, of about a factor of 3 in fatigue life. For notched parts the slope of the S - N curve on logarithmic scales is steeper, yielding more extreme changes. Thus, even small changes in applied alternating stress can have a significant effect on fatigue life.

Constant fatigue life diagrams relating σ_a and σ_m are often modeled, as shown schematically in Fig. 17, by using one of the S - N models from Fig. 16 and the modified Goodman or Morrow equations for mean stress. In Fig. 17, the intercepts, σ_{Nf} , at $\sigma_m = 0$ for a given life are found from the fully reversed, $R = -1$, modeled S - N curves. Modified Goodman straight lines are shown passing through these intercepts and the ultimate tensile strength, σ_b , in Fig. 4.17. For these finite fatigue lives, the modified Goodman or Morrow equations should have S_f replaced with S_{Nf} , for a given life. Using these equations and Basquin's equation for the fully reversed, $R = -1$, finite life region, gives the following equations:

$$\sigma_{Nf} = A \cdot (N_f)^B, \quad (7)$$

and

$$\frac{\sigma_a}{\sigma_{Nf}} + \frac{\sigma_m}{\sigma_b} = 1 \quad \text{or} \quad \frac{\sigma_a}{\sigma_{Nf}} + \frac{\sigma_m}{\sigma_{f\,fr}} = 1. \quad (8)$$

Either of Eqs. 8 along with Eq. 7 provides information to determine estimates of allowable S_a and S_m for a given fatigue life of unnotched parts. When Eqs. 7 and 8 are used, the S - N curve for a given mean stress is parallel to the fully reversed, $R = -1$, S - N curve, i.e., the slope, B , remains unchanged.

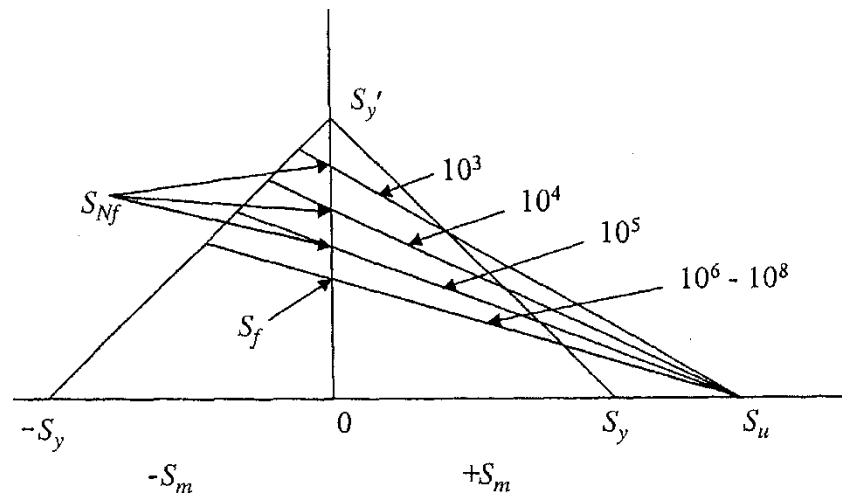


Figure 4.17 Constant life diagrams with superimposed yield criterion